SiliconPV 2023, 13th International Conference on Crystalline Silicon Photovoltaics
Silicon Material and Defect Engineering
https://doi.org/10.52825/siliconpv.v1i.842

Published: 22 Feb. 2024

Influence of AlO_x Interlayers on LeTID Kinetics in Ga-Doped Cz-Si

Joshua Kamphues[1][https://orcid.org/0000-0003-2575-1700], Andreas Schmid[1][https://orcid.org/0000-0003-2581-3975], Ronja Fischer-Süßlin[1][https://orcid.org/0009-0000-9454-7004], Giso Hahn[1][https://orcid.org/ 0000-0001-8292-1281], and Fabian Geml[1][https://orcid.org/ 0000-0002-2803-5390]

[1]University of Konstanz, Germany

Abstract. Light and elevated temperature-induced degradation (LeTID) is causing a reduction in efficiency especially in p-type silicon based solar cells. It is assumed to be strongly influenced by the hydrogen content in the bulk material. The presented work focuses on the impact of differently thick (5-25 nm) atomic layer-deposited aluminum oxide (AlO_x) interlayers underneath the hydrogen-rich silicon nitride (SiN_y:H) capping layer. The interlayer acts as a diffusion barrier for H during the firing step. It is demonstrated that the AlO_x interlayer has a comparable effect on the LeTID kinetics in Ga-doped Cz-Si (Cz-Si:Ga) as it is observed in B-doped Cz-Si (Cz-Si:B). Additionally, it substantially minimizes lifetime degradation in the Cz-Si:Ga sample. With a determined ratio of electron to hole capture cross sections k=26(3), the degradation phenomena are attributed to the LeTID kinetics. Deposition of AlO_x barrier layers exceeding 10 nm in thickness does not yield additional positive effects. Resistivity measurements revealed that the change in hole concentration correlates with the defect density for varying AlO_x layer thicknesses. The doping concentration seems to influence the change in maximum defect density for varying AlO_x layer thicknesses.

Keywords: Crystalline Silicon, Surface Passivation, Bulk Defects, Degradation, Hydrogen

1. Introduction

Light and elevated temperature-induced degradation (LeTID) is known to have a significant impact on the efficiency of crystalline silicon (c-Si) solar cells due to a decrease in the charge carrier lifetime [1]. This may be followed by a phase of regeneration [2]. It is very likely that H is a key factor responsible for LeTID in B-doped silicon and it has already been shown that the amount of H in the c-Si bulk can be reduced by an AlO_x layer beneath the SiN_y:H capping layer [3], [4], [5]. This could be explained by the AlO_x interlayer acting as a H diffusion barrier, which reduces the amount of H that diffuses into the c-Si during the firing step [6].

Ga-doped silicon does not suffer from BO-related degradation in B-doped c-Si but may suffer from LeTID [7], [8], [9], so it is very interesting to check its behavior concerning LeTID, as it is easier to be studied separately in this material. In this work, the influence of an AlO_x interlayer on the degradation of the effective excess charge carrier lifetime τ_{eff} in Czochralski (Cz)-grown c-Si (Cz-Si:Ga) is investigated by comparison with Cz-Si:B material. To gain more insights about the H content in the c-Si bulk, GaH- and BH-pairs are determined via resistivity measurements.

2. Experimental

Ga- (0.7 Ωcm and 1.8 Ωcm) and B-doped (2.0 Ωcm) Cz-Si material from LONGi, laser cut to a size of 5x5 cm², was used for τ_{eff} measurements. After removal of the saw damage and a cleaning process, atomic layer deposition (ALD) with a *FlexAL MK2* from *Oxford Instruments* was used to form AlO_x layers ranging between 5-25 nm in thickness at a deposition temperature of 300°C. Additionally, a reference sample group for each dopant was processed without an AlO_x barrier layer. All symmetrically processed samples received a SiN_y:H layer on both sides with a thickness of 75 nm using plasma-enhanced chemical vapor deposition (PECVD) in a machine from *Centrotherm*. All samples were fired at a measured peak sample temperature of 800°C in a belt furnace from *Centrotherm*.

Lifetime analysis was carried out at 30°C by the photoconductance decay method with a *Sinton Lifetime Tester WCT-120* after samples have been treated iso-generatively at 1.0(1) sun illumination and a temperature of 100°C for Ga- and B-doped samples. The measured τ_{eff} was used to calculate the lifetime equivalent defect density ΔN_{leq} for qualitative comparison of the different doping materials, as described in [10]. Photoconductive decay (PCD) measurements were used to determine τ_{eff} evaluated at an excess charge carrier density of $\Delta n = 0.1\ p_0$, with p_0 being the dopant concentration. For the Ga-doped samples an additional evaluation of the saturation current density j_0 was performed according to [11] and photoluminescence (PL) images were taken.

To determine the concentration of GaH- and BH-pairs by resistivity measurements [12], [13], Al was deposited in four lines on one side of the samples by electron-beam physical vapor deposition with a *Pfeiffer Classic 570 L* vacuum system, followed by laser fired contacting (LFC) with a *Rofin Powerline 100D*. B- and Ga-doped samples for resistivity measurements have been annealed at 180°C in the dark. Once the measured resistivity of Ga-doped samples saturated, a further treatment at 300(1)°C and 2.0(2) suns was performed.

3. Results and discussion

3.1 Comparison of defect densities for Ga- and B-doped samples

The upcoming results should only be interpreted qualitatively since the doping concentration between B- and Ga-doped samples vary. Therefore, only the lifetime equivalent defect density (ΔN_{leq}) will be compared to observe trends in the shown data.

The resulting ΔN_{leq} of the Cz-Si:Ga material with varying AlO_x barrier thickness is shown in Fig. 1 (a). Without any barrier layer between the H-rich SiN_y:H and the c-Si bulk, ΔN_{leq} is increasing for the first few minutes of the treatment. After reaching the maximum ΔN_{leq}, regeneration can be observed. With the addition of the AlO_x interlayer beneath the SiN_y:H with a thickness of 5-25 nm, the observed defect density is lowered. For better visibility, a fitting with three exponential functions is added to the data points. There is no further reduction of the defect density visible for an AlO_x interlayer with a thickness >10 nm. The capture cross-section ratio k for the defect after roughly one day of degradation is calculated to k = 26(3) which seems to be in good accordance with the literature [14]. The time constants from the exponential fitting are determined as t_1=0.35(4) h, t_2=15(4) h, t_3=23(6) h and present a degradation with a following regeneration of the Ga-doped material. Starting lifetimes for these samples are between 300 µs and 600 µs.

The saturation current density is evaluated to monitor surface degradation. Fig. 1 (b) illustrates j_0 for the Ga-doped samples subjected to 100°C, 1.0 sun. Samples with an AlO_x interlayer are evaluated using the standard slope-based method. In the case of the reference sample, this evaluation results in an underestimation of j_0. To address this issue, a new difference

analysis method is used [15]. All samples maintained a relatively constant j_0 during degradation, indicating that the degradation of τ_{eff} is a bulk related phenomenon mainly caused by LeTID kinetics as it is observable for ΔN_{leq} in Fig. 1 (a). However, the sample without any interlayer exhibits an increase of j_0 after approximately 100 h pointing towards a degradation of surface passivation quality.

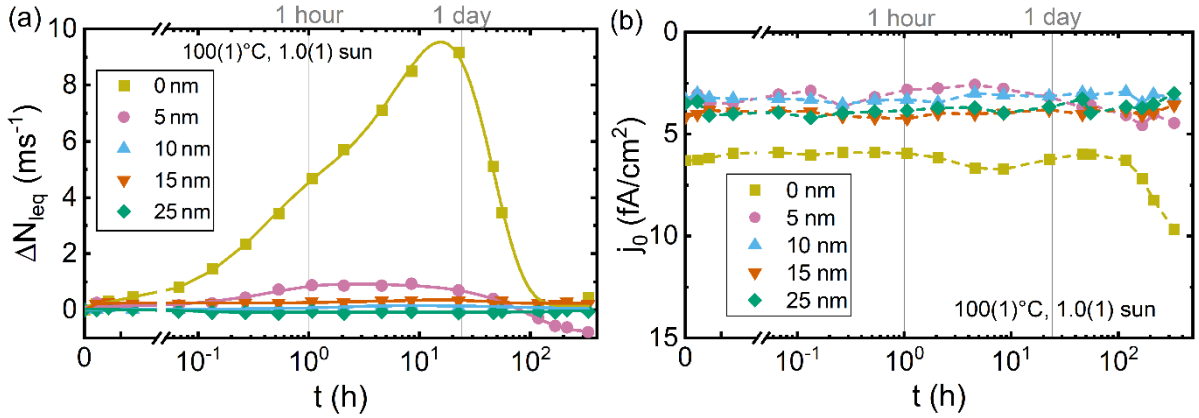

Figure 1. (a) ΔN_{leq} over accumulated time during iso-generative degradation at 100°C, 1.0(1) sun in Cz-Si:Ga (0.7 Ωcm) (b) Corresponding saturation current density j_0, with dashed lines as guide for the eyes, over the accumulated time at 1.0(1) sun at 100°C for the 0.7 Ωcm Ga-doped samples.

Additionally, PL images for the degradation of the Ga-doped samples are shown in Fig. 2. The sample without AlO_x interlayer shows a significant degradation after 22.5 h (time of maximum degradation of the sample without AlO_x layer), which is consistent with the results obtained from ΔN_{leq} measurements. In contrast, there is barely any degradation visible for the samples with an AlO_x layer. However, it should be noted that the injection is higher for the evaluation with PL compared to PCD with $\Delta n = 0.1\ p_0$, resulting in less pronounced differences. This could be the reason no visible degradation is observed for the sample with a 5 nm AlO_x interlayer. All samples keep their homogeneity during the illuminated treatment.

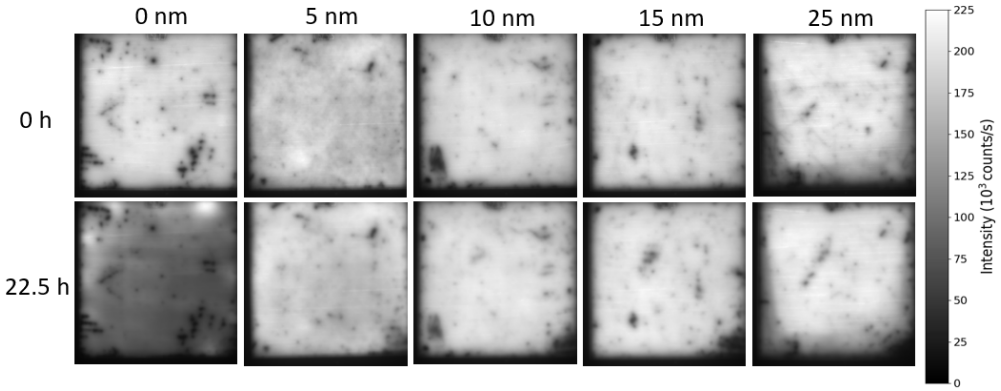

Figure 2. PL images of the Cz-Si:Ga (0.7 Ωcm) samples with various AlO_x interlayer thicknesses before degradation (top) and after 22.5 h of illumination at 1.0(1) sun and 100°C (bottom).

For a direct comparison, similarly doped Cz-Si:Ga (1.8 Ωcm) and Cz-Si:B (2.0 Ωcm) samples are processed and treated under the same conditions. Fig. 3 shows the defect density for Ga- and B-doped samples with varying AlO_x interlayer thicknesses over the accumulated time during treatment at 1.0(1) sun iso-generative illumination at 100(1)°C. The defect density ΔN_{leq} for the B-doped samples is significantly higher ($\Delta N_{leq,max}$ >20 ms^{-1}) compared to the Ga-doped samples ($\Delta N_{leq,max}$ <3 ms^{-1}). With the increasing thickness of the AlO_x interlayer, a decrease in

the defect density is observed for both Ga- and B-doped samples, but the relative decrease is more significant for the Ga-doped samples as it was already observed in Fig. 1 (a). The reference samples for each dopant without interlayer exhibit another increase in defect density after roughly 40 h of treatment, which can again be related to the degradation of surface passivation.

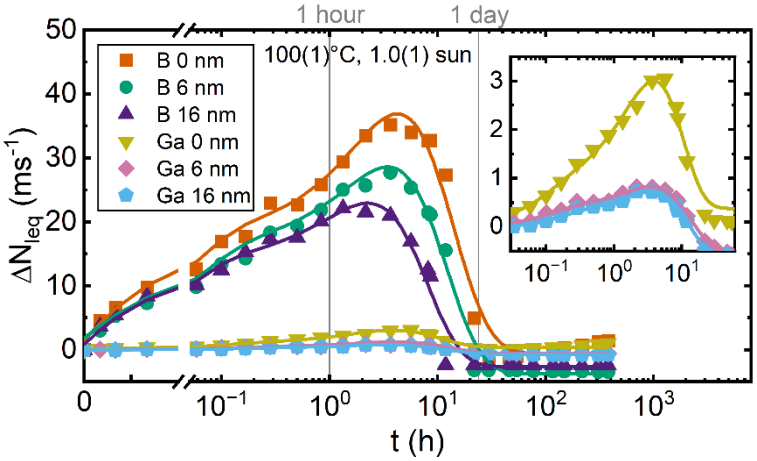

Figure 3. Direct comparison of defect densities ΔN_{leq} over accumulated time during iso-generative degradation at 1.0(1) sun for Cz-Si:B (2.0 Ωcm) and Cz-Si:Ga (1.8 Ωcm) with AlO_x interlayers of 6 nm and 16 nm and a reference, respectively.

It is likely that the effect of the reduced H diffusion from the SiN_y:H layer into the c-Si bulk affects the LeTID kinetics in the Cz-Si:Ga similarly to the kinetics in Cz-Si:B. Further experiments, determining the concentration of GaH- and BH-pairs by resistivity measurements to gain more insights regarding the H content in the bulk, will be discussed in the next section.

3.2 Determination of GaH- and BH-pairs via resistivity measurements

The H content in Ga- and B-doped samples is investigated by the determination of GaH- and BH-pairs via resistivity measurements. This involves a process whereby H_2 dimers dissociate and form GaH- and BH-pairs with the corresponding dopant species, which results in a depletion of holes and thus an increase in resistivity. Fig. 4 displays changes in hole concentration during dark anneal at 180(1)°C (left) followed by illumination at 2.0(2) suns at 300(1)°C (right) over the accumulated treatment time for Cz-Si:Ga (0.7 Ωcm) considering different AlO_x layer thicknesses. It can be observed that the maximum of the change in hole concentration saturates at around 2.5×10^{14} cm^{-3} for an AlO_x interlayer exceeding 10 nm in thickness. This observation aligns with the findings on defect densities presented in Fig. 1 (a).

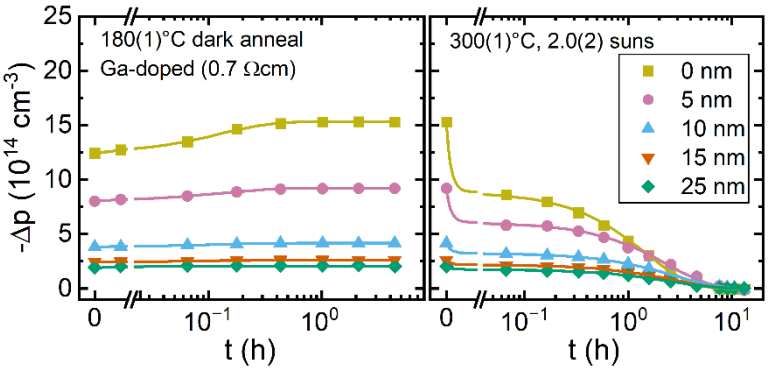

Figure 4. Change in hole concentration Δp over accumulated time during dark anneal at 180°C (left) and illumination (2.0 suns, 300°C) (right) for Cz-Si:Ga (0.7 Ωcm) samples with varying AlO_x layer thickness between 5-25 nm and a reference without interlayer.

Comparable samples to those presented in Fig. 3 underwent resistivity measurements to identify GaH-pairs in the 1.8 Ωcm Ga-doped material and BH-pairs in the 2 Ωcm B-doped material. The observed association and dissociation of GaH- (a) and BH- (b) pairs through changes in hole concentration over accumulated time across varying AlO_x interlayer thicknesses is depicted in Fig. 5. For both types of dopants, a similar trend is observable but the maximum Δp is lower for B-doped samples. Comparing the resistivity measurements of the 0.7 Ωcm Ga-doped material in Fig. 4 with the 1.8 Ωcm doped material in Fig. 5 (a) indicates a different behavior for variations of the AlO_x barrier thickness.

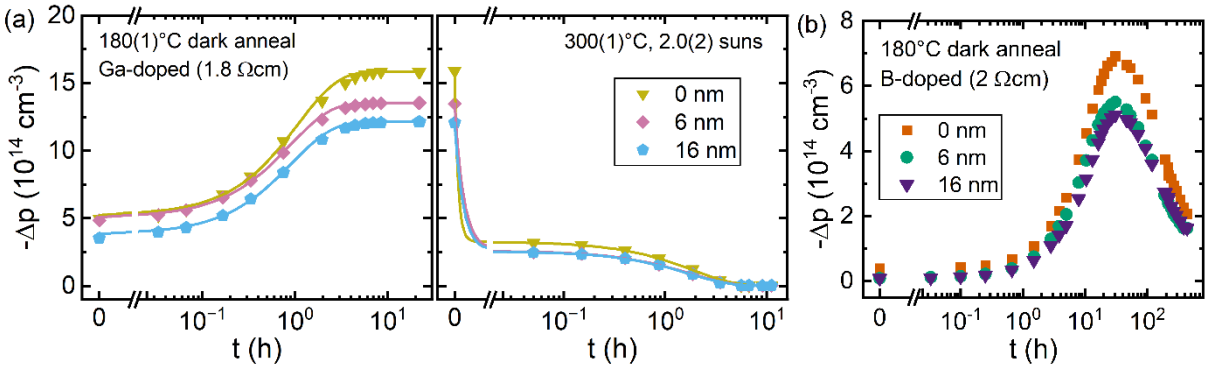

Figure 5. Change in hole concentration Δp over accumulated time for Cz-Si:Ga (1.8 Ωcm) during dark anneal at 180°C on the left and illumination at 300°C on the right (a) and Cz-Si:B during dark anneal at 180°C (b) for AlO_x interlayers of 6 nm and 16 nm compared to a reference sample without interlayer.

3.3 Qualitative analysis of the influence of AlO_x thickness on ΔN_{leq} and Δp

Finally, Fig. 6 summarizes the results on resistivity and lifetime equivalent defect densities by comparing the maximum defect densities $\Delta N_{leq,max}$ (left scale) with the maximum change in hole concentration Δp_{max} (right scale) depending on the thickness of applied AlO_x interlayer for all materials used in this work.

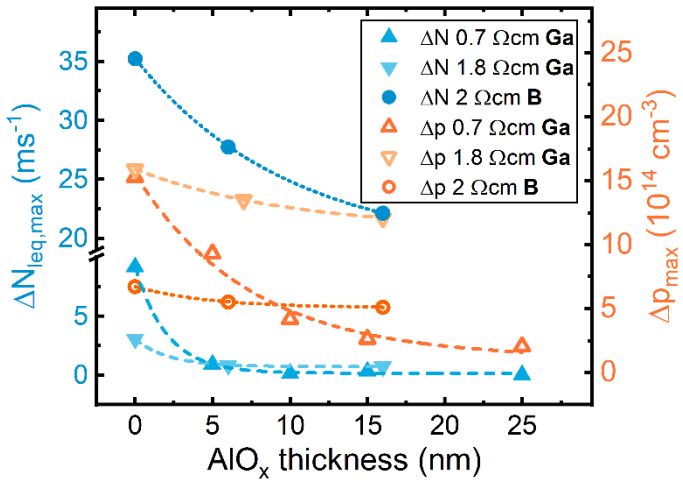

Figure 6. Maximum defect densities (at 100°C, 1 sun) and maximum change in hole concentration for all samples fired at a measured peak temperature of 800°C in dependence of the AlO_x interlayer thickness.

This representation enables a comparison between defect densities of differently doped Ga-doped and B-doped samples with their corresponding maximum GaH- and BH-pair association. In addition, the comparison is limited to samples that were specifically prepared for this

research to ensure consistency of preparation and measurement procedures across different materials. Note that all lifetime samples are treated under 1 sun illumination at 100°C, and therefore reaction equilibriums might change for different doping concentrations. Based on the data presented, it appears that defect densities are higher in B-doped samples compared to those doped with Ga. Additionally, it seems that the behavior of defect density and change in hole concentration with increasing AlO_x thickness is influenced by the doping concentration which can be observed by the change in steepness for the two doping concentrations of Ga-doped samples. Notably, in the case of B-doped material, saturation of $\Delta N_{leq,max}$ is not observed until a layer thickness of 16 nm, which contrasts with the observed saturation in resistivity measurements for AlOx layers thicker than 6 nm.

The decline in $\Delta N_{leq,max}$ for increased barrier thicknesses is steeper than the decline in Δp_{max} for all samples. This aligns with previous findings that the amount of H is not the only factor influencing the defect density and that other mechanisms may become a dominant factor as the barrier thickness increases. Furthermore, a crossover between the 2 Ωcm B-doped material and the 0.7 Ωcm Ga-doped material around an interlayer thickness of 10 nm appears. For the 1.8 Ωcm Ga-doped material this cannot be observed. Surprisingly, the amount of GaH-pairs in the maximum associated state is almost the same for the two doping concentrations in Ga-doped samples. Another observation is that the saturation of Δp_{max} is only visible for layer thicknesses exceeding 15 nm for the 0.7 Ωcm Ga-doped samples. In case of the defect density, a saturation is visible for AlO_x layers exceeding 10 nm in thickness. It should be noted that this research only considers a limited range of materials and interlayer thicknesses, which makes it difficult to draw general conclusions about how these parameters influence defect formation.

4. Conclusion

In conclusion, the present study shows the impact of AlO_x barrier thickness on the defect densities and hydrogen content in Cz-Si:B and Cz-Si:Ga materials under LeTID conditions. Defect density and surface-related degradation are strongly reduced by the implementation of an AlO_x interlayer between the bulk material and the SiN_y:H for Cz-Si. Moreover, the Ga-doped samples (1.8 Ωcm) exhibit a lower defect density compared to B-doped samples under 1.0(1) sun at 100(1)°C which is in contrast to Δp_{max}. Determinations of GaH- and BH-pairs by resistivity measurements reveal that the amount of H correlates with the observed ΔN_{leq} for B- and Ga-doped materials. The decline in maximum defect densities with increasing barrier thickness is steeper than the decline in maximum change in hole concentration. Saturation of maximum change in hole concentration is visible for 0.7 Ωcm Ga-doped samples with layer thicknesses >15 nm, while saturation of defect density is visible for AlO_x layers >10 nm. Further investigations regarding the influence of various doping concentrations on H content and LeTID dynamics should be executed.

Data availability statement

The data that support the findings of this study are available from the corresponding author upon reasonable request.

Author contributions

J. Kamphues: formal analysis, investigation, validation, visualization, conceptualization, writing - original draft; **A. Schmid:** Investigation, formal analysis, software; **R. Fischer-Süßlin:** investigation; **G. Hahn:** funding acquisition, project administration, resources, supervision, writing – review & editing; **F. Geml:** project administration, conceptualization, supervision, writing – review & editing

Competing interests

The authors declare that they have no competing interests.

Funding

Part of this work was financially supported by the German Federal Ministry for Economic Affairs and Climate Action (FKZ 03EE1102C). The content is the responsibility of the authors.

Acknowledgement

The author would like to thank Jochen Simon for in-depth discussion about the formation of GaH pairs and Axel Herguth for insights about the evaluation of j_0.

References

1. F. Kersten, P. Engelhart, H.C. Ploigt, A. Stekolnikov, T. Lindner, F. Stenzel, M. Bartzsch, A. Szpeth, K. Petter, J. Heitmann, J. W. Müller, “Degradation of multicrystalline silicon solar cells and modules after illumination at elevated temperature”, Solar Energy Materials and Solar Cells, vol.142, pp. 83-86, 2015, doi: https://doi.org/10.1016/j.solmat.2015.06.015
2. A. Zuschlag, D. Skorka, G. Hahn, “Degradation and regeneration analysis in mc-Si”, in Proc. 43rd IEEE PVSC, 2016, pp. 1051-1054, doi: https://doi.org/10.1109/PVSC.2016.7749772
3. N.E. Grant, J.R. Scowcroft, A. I. Pointon, M. Al-Amin, P.P. Altermatt, J.D. Murphy, “Lifetime instabilities in gallium doped monocrystalline PERC silicon solar cells”, Solar Energy Materials and Solar Cells, vol.206, pp. 110299, 2020, doi: https://doi.org/10.1016/j.solmat.2019.110299
4. A. Schmid, C. Fischer, D. Skorka, A. Herguth, C. Winter, A. Zuschlag, G. Hahn, “On the role of AlO_x thickness in AlO_x/SiN_y:H layer stacks regarding light- and elevated temperature-induced degradation and hydrogen diffusion in c-Si”, IEEE Journal of Photovoltaics, vol.11, no.4, pp. 967-973, 2021, doi: https://doi.org/10.1109/JPHOTOV.2021.3075850
5. L. Helmich, D. C. Walter, D. Bredemeier, J. Schmidt, “Atomic-layer-deposited Al_2O_3 as effective barrier against the diffusion of hydrogen from SiN_x:H layers into crystalline silicon during rapid thermal annealing”, Physica Status Solidi RRL, vol.14, p. 2000367, 2020, doi: https://doi.org/10.1002/pssr.202000367
6. S. Wilking, A. Herguth, G. Hahn, “Influence of hydrogen on the regeneration of boron-oxygen related defects in crystalline silicon”, Journal of Applied Physics, vol.113, p. 194503, 2013, doi: https://doi.org/10.1063/1.4804310
7. U. Varshney, B. Hallam, P. Hamer, A. Ciesla, D. Chen, S. Liu, C. Sen, A. Samadi, M. Abbott, C. Chan, B. Hoex, “Controlling light- and elevated-temperature-induced degradation with thin film barrier layers”; IEEE Journal of Photovoltaics, vol.10, no.1, pp. 19-27, 2020, doi: https://doi.org/10.1109/JPHOTOV.2019.2945199
8. M. Winter, D.C. Walter, B. Min, R. Peibst, R. Brendel, J. Schmidt, „Light and elevated temperature induced degradation and recovery of gallium-doped Czochralski-silicon solar cells”, scientific reports, vol.12, p. 1-8, 2022, doi: https://doi.org/10.1038/s41598-022-11831-3
9. S. Jafari, Z. Hameiri, “Investigation of light-induced Degradation in Ga- and In-doped Cz silicon”, IEEE 48th Photovoltaic Specialists Conference, pp.814-817, 2021, doi: https://doi.org/10.1109/PVSC43889.2021.9518574
10. A. Herguth, “On the lifetime-equivalent defect density: properties, application, and pitfalls”, IEEE Journal of Photovoltaics, vol.9, no.5, pp. 1182-1194, 2019, doi: https://doi.org/10.1109/JPHOTOV.2019.2922470

11. A. Kimmerle, J. Greulich, A. Wolf, “Carrier-diffusion corrected J_0-analysis of charge carrier lifetime measurements for increased consistency”, Solar Energy Materials and Solar Cells, vol.142, pp. 116-122, 2015, doi: https://doi.org/10.1016/j.solmat.2015.06.043
12. A. Herguth, C. Winter, “Methology and error analysis of direct resistance measurements used for the quantification of boron-hydrogen pairs in crystalline silicon”, IEEE Journal of Photovoltaics, vol.11, no.4, pp. 1059-1068, 2021, doi: https://doi.org/10.1109/JPHOTOV.2021.3074463
13. J. Simon, A. Herguth, L. Kutschera, G. Hahn, “The dissociation of gallium-hydrogen pairs in crystalline silicon during illuminated annealing”, Physica Status Solidi RRL, vol.16, no.12, p. 2200297, 2022, https://doi.org/10.1002/pssr.202200297
14. D. Lin, Z. Hu, L. Song, D. Yang, X. Yu, “Investigation on the light and elevated temperature induced degradation of gallium-doped Cz-Si”, Solar Energy, vol.225, pp. 407-411, 2021, doi: https://doi.org/10.1016/j.solener.2021.07.023
15. A. Herguth, J. Kamphues, “On the impact of bulk lifetime on the quantification of recombination at the surface of semiconductors”, IEEE Journal of Photovoltaics, vol.13, no.5, pp. 672-681, 2023, doi: https://doi.org/10.1109/JPHOTOV.2019.2945199